

Relations between integrated and monochromatic luminosities of flat-spectrum radio quasars *

Zhi-Fu Chen¹, Zhao-Yu Chen², Yi-Ping Qin^{1,4}, Min-Feng Gu³, Lian-Zhong Lü⁴,
Cheng-Yue Su⁵, You-Bing Li⁶ and Ye Chen¹

¹ Center for Astrophysics, Guangzhou University, Guangzhou 510006, China;
zhichenfu@gmail.com

² Department of Astronomy, Peking University, Beijing 100871, China

³ Key Laboratory for Research in Galaxies and Cosmology, Shanghai Astronomical Observatory,
Chinese Academy of Sciences, Shanghai 200030, China

⁴ Physics Department, Guangxi University, Nanning 530004, China

⁵ Department of Physics, Guangdong University of Technology, Guangzhou 530004, China

⁶ Guangzhou City Construction College, Guangzhou 530004, China

Received 2010 July 9; accepted 2010 November 24

Abstract We employ a sample of 362 flat-spectrum radio quasars (FSRQs) to calculate their integrated luminosities by integrating the spectral energy distribution (SED) constructed with multi-band (radio, IR, optical, UV and X-ray) data. We compare these luminosities with those estimated from monochromatic luminosities by multiplying them by the conventional bolometric correction factors. Our analysis shows that the integrated luminosities calculated from the SED are much larger than the bolometric luminosities estimated from monochromatic luminosities. Their departing behavior tightly correlates with radio luminosities. The relations between integrated and monochromatic luminosities are explored, which are regarded as empirical relations that might be more suitable to be applied to estimate integrated luminosities of FSRQs from their monochromatic luminosities.

Key words: methods: statistical — galaxies: active — galaxies: jets

1 INTRODUCTION

Quasars belong to the most luminous subclass of Active Galactic Nuclei (AGNs), with nuclear magnitudes being $M_B < -21.5 + 5 \log h_0$ (Peterson 1997). A small minority (5% ~ 10%) of these objects are strong radio sources. Following Miller et al. (1990), quasars can be divided into radio-loud quasars (whose 1.4 GHz luminosities are greater than $10^{25} \text{ W Hz}^{-1}$) and radio-quiet quasars (whose 1.4 GHz luminosities are smaller than $10^{25} \text{ W Hz}^{-1}$). Using radio spectral index α ($f \propto \nu^{-\alpha}$), we can also divide radio-loud quasars into steep spectrum radio quasars (SSRQs, $\alpha > 0.5$) and flat spectrum radio quasars (FSRQs, $\alpha < 0.5$). FSRQs constitute the most extreme class of AGNs, characterized by their apparent superluminal motion, strong and rapid variability and high polarization.

* Supported by the National Natural Science Foundation of China.

These extreme properties are generally interpreted as the result of the orientation of the relativistic jet close to the line of sight.

The integrated luminosity emitted from an AGN is one of its basic parameters. However, it is also one of the most difficult parameters to determine. It requires ground-based and space-based observational data to construct a spectral energy distribution (SED). Generally, the bolometric luminosity (L_{bol}) is approximated from the integrated luminosity (L_{SED}) which spans many decades in wavelength (Woo & Urry 2002). For the radio-quiet quasars, the thermal emission is dominant. Therefore, L_{SED} could approximately represent L_{bol} . For the extremely radio-loud quasars (FSRQs), however, the non-thermal emission of relativistic jets significantly contributes to all frequencies (Urry & Padovani 1995, Wu et al. 2004, Wu 2009). Thus, their L_{SED} values are much greater than their L_{bol} values.

Generally, the L_{bol} values are estimated from monochromatic luminosities by multiplying the corresponding bolometric correction factors. For example, Kaspi et al. (2000), Netzer (2003), Wu & Liu (2004), Peterson et al. (2004), Woo et al. (2006), Kollmeier et al. (2006), Kim et al. (2008) and Lu et al. (2010) calculated L_{bol} with $L_{\text{bol}} = 9\lambda L_{\lambda}(5100 \text{ \AA})$. Here, they assumed that the AGN spectral energy distribution comes from typical optically-selected quasars with little dust obscuration and hence adopted a bolometric correction factor of 9. Meanwhile, Warner et al. (2004) preferred bolometric correction factors of 4.36 and 9.27 for continuum monochromatic luminosity at 1450 Å and 5100 Å, respectively, while McLure & Dunlop (2004) adopted bolometric correction factors of 5.9 and 9.8 for continuum monochromatic luminosity at 3000 Å and 5100 Å respectively for the 1136 Sloan Digital Sky Survey (SDSS) quasars whose spectra cover both 5100 Å and 3000 Å.

The value of L_{bol} can also be estimated by broad line region luminosity using the empirical relation $L_{\text{bol}} = f^{-1}L_{\text{BRL}}$, where f is the covering factor of the broad line region. The value of f is not well established. It is generally taken from 5% to 30% (Maiolino 2001), and its typical value is $\sim 10\%$ (Netzer 1990; Peterson 1997).

The reason for estimating bolometric luminosity with the bolometric correction factor or empirical relation is that the integration of the SED is usually hampered by the lack of integrated wavelength coverage. Generally, the bolometric correction factors are calculated by a composite SED. Several previous studies of quasar SEDs have been published. The work of Edelson & Malkan (1986) included an SED for IRAS bright AGNs; Ward et al. (1987) worked on hard X-ray selected Seyfert galaxies; Sanders et al. (1989) presented an infrared to optical SED for PG quasars and Sun & Malkan (1989) presented a near-infrared to ultraviolet SED for IUE observed quasars. Woo & Urry (2002) constructed an average SED using various sources: radio-loud and radio-quiet quasars were from Elvis et al. (1994); Serfert 1 studies were from Mas-Hesse et al. (1995) and Serfert 2 studies were from Schmitt et al. (1997). They found that the bolometric luminosities are roughly 10 times the optical luminosities.

Elvis et al. (1994) have presented the bolometric correction factors which were derived from the mean spectral energy distribution (MED) of normal, nonblazar quasar cases. However, they noted that the dispersion is large. Recently, Richards et al. (2006) showed the bolometric corrections in their paper, which were derived from the composite SED. They also pointed out that the bolometric corrections and bolometric luminosities are obtained by assuming that quasars emit isotropically, but the assumption is not acceptable.

Nevertheless, in the above bolometric corrections, the particular properties of extremely radio-loud AGNs are not taken into account. Due to the contribution of the emission of relativistic jets, the integrated luminosities of extremely radio-loud quasars are much greater than the bolometric luminosities estimated by monochromatic luminosities using bolometric correction factors of normal quasars for FSRQs (Wu et al. 2004). For FSRQs, we expect that the departure of the integrated luminosities from the bolometric luminosities estimated by monochromatic luminosities using bolometric correction factors of normal quasars may be influenced by the emission of relativistic jets. In this paper, we will investigate the relationship between the departure and the emission of relativistic

tic jets. We will also derive the relations between the integrated luminosities and monochromatic luminosities for FSRQs, which might be different from those of normal quasars.

Throughout this paper, we adopt a flat cosmology with $\Omega_M = 0.26$, $\Omega_\Lambda = 0.74$ and $h = 0.71$ (Spergel et al. 2007).

2 DATA AND SAMPLES

Our sample is selected based on the cross-identification of the X-ray emitting SDSS broad line AGN catalog (Anderson et al. 2007), the radio catalog of the FIRST 20 cm survey (White et al. 1997) and the GB6 survey (Gregory et al. 1996). In their analysis, Anderson et al. (2007) employed X-ray data from the ROSAT All Sky Survey (RASS) and both optical imaging and spectroscopic data from SDSS. The X-ray emitting SDSS broad line AGN sources are required to have at least one emission line with full width at half-maximum (FWHM) larger than 1000 km s^{-1} and with highly reliable redshifts (Anderson et al. 2007). The RASS/SDSS data from the 5740 deg^2 of sky spectroscopically covered in SDSS DR 5 provide an expanded catalog of 7000 confirmed quasars and other AGNs that are probably RASS identifications (Anderson et al. 2007). We build a RASS-SDSS-FIRST-GB6 cross-identified FSRQ sample of 362 quasars with radio spectral index $\alpha < 0.5$ ($f \propto \nu^{-\alpha}$) by cross-identifying the broad-line AGN catalog of Anderson et al. (2007) and the FIRST and GB6 radio-detected sources. The 2 keV X-ray luminosity in the source rest frame based on the X-ray emitting SDSS broad line AGN catalog is obtained by assuming a power-law X-ray spectrum with energy index $\alpha_X = 1.5$, and is corrected for the absorption of the Galaxy, with X-ray-absorbing columns being estimated using the N_H column-density measures of the Stark et al. (1992) 21 cm maps (Anderson et al. 2007).

First, we cross-correlate the X-ray emitting SDSS broad line AGN catalog with the FIRST catalog within 5 arcsec and the GB6 catalog within 1 arcmin (Kimball & Ivezić 2008, Chen et al. 2009). To get multi-band data, we take the infrared photometric magnitudes of J , H and K_s bandpasses provided by 2MASS (Skrutskie et al. 2006), and pick out the sources by cross-correlating them with 2MASS within a matched radius of 2 arcsec (Schneider et al. 2010). Then, we collect the Far- and near-UV magnitudes from the Galaxy Evolution Explorer (GALEX; Martin et al. 2005) matched within 5 arcsec of SDSS positions (Budavári et al. 2009). In order to construct the SED, we adopt SDSS point-spread function (PSF) magnitudes (u , g , r , i , z) for the optical data. The magnitudes of IR (J , H , K_s), optical (u , g , r , i , z) and UV (far-UV, near-UV) are corrected for Galactic extinction using the reddening maps of Schlegel et al. (1998), and their K-corrections are performed. We also make K-corrections for radio luminosities. We fit the SED with a parabola (Sambruna et al. 1996), and then integrate the parabola to obtain the integrated luminosity of the SED (L_{SED}).

The sample in Shen et al. (2008) is an extension of the published SDSS DR5 quasar catalog (Schneider et al. 2007), which contains 77 429 quasars that have luminosities larger than $M_i = -22.0$ and have at least one broad emission line ($\text{FWHM} > 1000 \text{ km s}^{-1}$) or have interesting/complex absorption features (see Schneider et al. 2007 for details). The continuum monochromatic luminosities at rest frame 5100 Å, 3000 Å and 1350 Å, which depend on redshift, have been measured after correcting for Galactic extinction using the reddening maps of Schlegel et al. (1998). The authors have also calculated the bolometric luminosity (L_{Shen}) with bolometric correction factors: $\text{BC}_{5100 \text{ Å}} = 9.26$, $\text{BC}_{3000 \text{ Å}} = 5.15$ and $\text{BC}_{1350 \text{ Å}} = 3.18$ (see Shen et al. 2008 for details). For the continuum monochromatic luminosities at rest frame 5100 Å, 3000 Å and 1350 Å in our sample of 362 FSRQs, we consider those values directly taken from Shen et al. (2008).

The luminosities of each bandpass (1.4 GHz, 4.85 GHz, J, H, K, FUV, NUV) and integrated luminosity of SED are listed in Table 1. Its entirety is published in the electronic edition (see the RAA's webpage) A portion is shown here for guidance regarding its form and content.

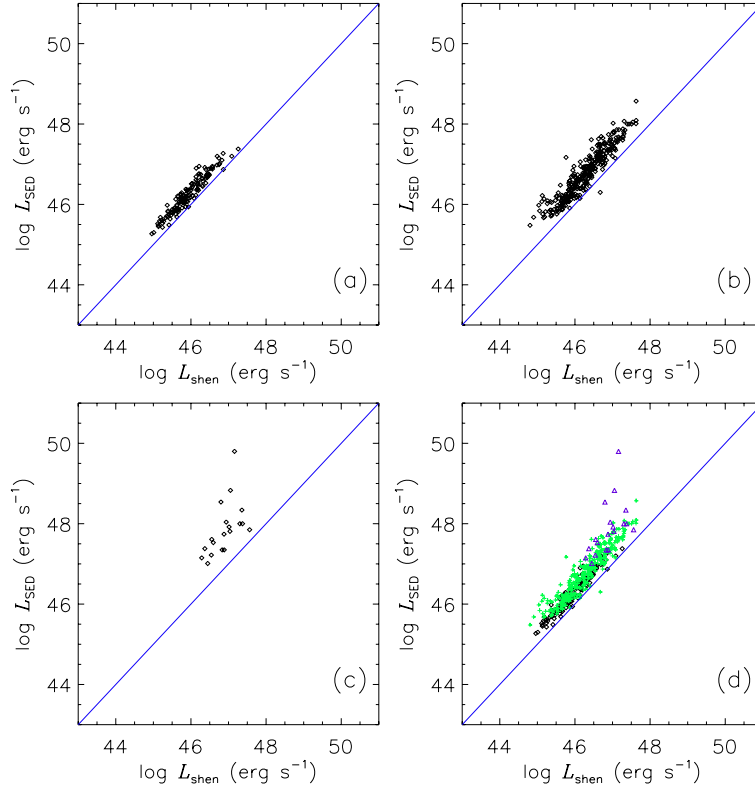


Fig. 1 L_{SED} versus L_{Shen} . (a) L_{Shen} are calculated by continuum monochromatic luminosities, at 5100 Å, using correction factor $\text{BC}_{5100 \text{ \AA}}^{\circ}=9.26$; (b) L_{Shen} are calculated by continuum monochromatic luminosities, at 3000 Å, using correction factor $\text{BC}_{3000 \text{ \AA}}^{\circ}=5.15$; (c) L_{Shen} are calculated by continuum monochromatic luminosities, at 1350 Å, using correction factor $\text{BC}_{1350 \text{ \AA}}^{\circ}=3.18$; (d) L_{Shen} are calculated by continuum luminosities at 5100 Å (black), 3000 Å (green) and 1350 Å (blue), respectively. The blue solid lines indicate that the L_{Shen} values are equal to L_{SED} .

Table 1 Observation Parameters

SDSS name	z	$\log L_{\text{SED}}$	$f_{1.4}$	error	$f_{4.85}$	error	J	error	H	error	K	error	FUV	error	NUV	error
(1)	(2)	(3)	(4)	(5)	(6)	(7)	(8)	(9)	(10)	(11)	(12)	(13)	(14)	(15)	(16)	(17)
001130.40+005751.7	1.4934	46.65	149.07	14.91	140	14	0.00	0.00	0.00	0.00	15.97	0.29	0.00	0.00	0.00	0.00
013352.66+011345.1	0.3081	45.64	8.53	0.85	60	8	16.63	0.19	15.55	0.15	14.93	0.13	18.79	0.03	18.66	0.02
021225.56+010056.1	0.5128	46.18	18.34	1.83	51	8	16.98	0.23	0.00	0.00	15.23	0.18	18.95	0.13	18.50	0.06
073320.83+390505.1	0.6637	46.44	117.16	11.72	100	9	17.34	0.32	0.00	0.00	15.91	0.25	19.48	0.10	18.76	0.04
073422.19+472918.8	0.3819	45.86	6.47	0.65	96	9	16.30	0.12	15.76	0.18	14.82	0.10	0.00	0.00	22.50	0.36
074218.21+194719.4	0.6573	46.67	51.54	5.15	57	6	16.86	0.17	15.94	0.17	15.25	0.14	19.27	0.03	18.06	0.01
074237.38+394435.6	2.2007	47.38	106.26	10.63	123	11	0.00	0.00	0.00	0.00	0.00	0.00	0.00	0.00	0.00	0.00
074242.18+374402.0	0.8057	46.59	13.97	1.40	37	5	17.31	0.29	0.00	0.00	16.02	0.26	22.74	0.21	20.00	0.04
074344.97+232838.9	0.7766	46.73	107.82	10.78	196	18	16.16	0.08	16.00	0.14	15.34	0.13	20.26	0.16	18.87	0.05
074541.66+314256.6	0.4609	47.05	614.64	61.46	941	83	14.48	0.03	13.78	0.03	12.95	0.03	17.26	0.05	16.50	0.01
...

(1) SDSS name, (2) Redshift, (3) $\log L_{\text{SED}}$ in units of erg s^{-1} , (4) ~ (7): observed flux and flux error for 1.4 GHz and 4.85 GHz in units of mJy, (8) ~ (17): observed magnitude and magnitude error for J , H , K , FUV and NUV in units of mag.

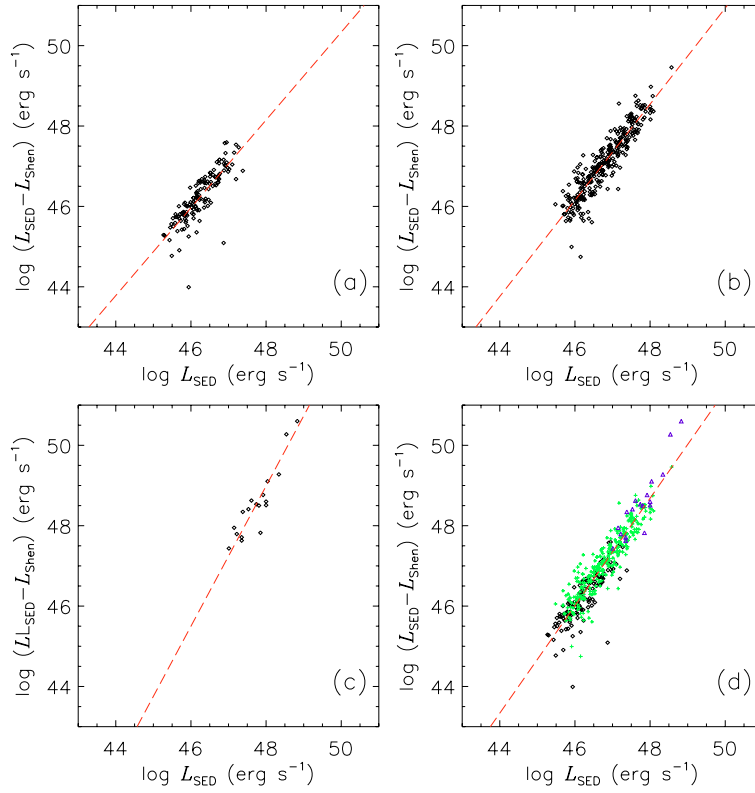


Fig. 2 Departures between L_{SED} and L_{Shen} versus L_{SED} . (a) L_{Shen} are calculated by continuum monochromatic luminosities at 5100 Å; (b) L_{Shen} are calculated by continuum monochromatic luminosities at 3000 Å; (c) L_{Shen} are calculated by continuum monochromatic luminosities at 1350 Å; (d) L_{Shen} are calculated by continuum monochromatic luminosities at 5100 Å (black), 3000 Å (green) and 1350 Å (blue), respectively. The red dashed line is the minimum χ^2 fitting.

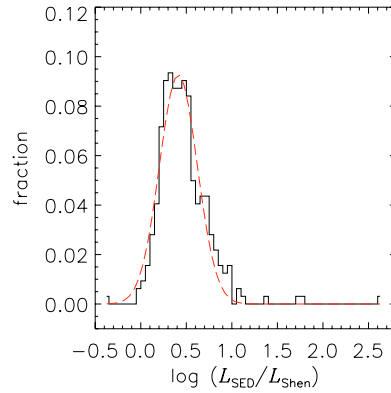


Fig. 3 Distribution of the departures between L_{SED} and L_{Shen} . The dashed curve is a Gaussian fitting with mean and dispersion 0.413 and 0.207 respectively.

3 RESULTS AND DISCUSSION

The integrated luminosity emitted by an AGN includes both thermal and non-thermal emissions. The thermal emission and bolometric luminosity can be estimated by monochromatic luminosity using bolometric correction factors. For radio-quiet quasars, the non-thermal emission is weak, and therefore, the integrated luminosity approximates the bolometric luminosity. Namely, we can estimate the overall luminosity from monochromatic luminosity by simply multiplying the latter with the corresponding bolometric correction factor. However, for extremely radio-loud quasars, if we estimate the integrated luminosities from monochromatic luminosities by multiplying bolometric correction factors drawn from radio-quiet quasars, the results will be smaller than the true values since the non-thermal emission is strong.

Figure 1 compares the integrated luminosities with the bolometric luminosities (L_{Shen}) for the same objects in our sample. The figure clearly shows that, for the same objects, the bolometric luminosities are significantly smaller than their integrated luminosities. The departure between the integrated luminosities and the bolometric luminosities is plotted in Figure 2. It is clearly revealed in Figure 2 that the brighter the object, the larger the departure. The largest departure is up to $10^{52.44} \text{ erg s}^{-1}$ at $L_{\text{SED}} = 10^{49.80} \text{ erg s}^{-1}$ and the smallest departure is merely $10^{43.99} \text{ erg s}^{-1}$ at $L_{\text{SED}} = 10^{45.94} \text{ erg s}^{-1}$, while the arithmetical mean departure of the sample is $10^{47.07} \text{ erg s}^{-1}$. A minimum χ^2 fit to the departure and L_{SED} gives (see Fig. 2(a))

$$\log(L_{\text{SED}} - L_{\text{Shen}}) = (-20.80 \pm 1.16) + (1.45 \pm 0.02) \log(L_{\text{SED}}). \quad (1)$$

The histogram of the departure is shown in Figure 3. The mean and dispersion of the Gaussian are 0.413 and 0.207, respectively.

For extremely radio-loud quasars, the non-thermal emission of the relativistic jet significantly contributes to all frequencies (Urry & Padovani 1995, Wu et al. 2004, Wu 2009), and therefore it is reasonable that the integrated luminosities are much greater than the bolometric luminosities for these objects.

Elvis et al. (1994) have derived the mean bolometric correction factor at the V -band (5400 Å) for normal, nonblazar quasars (radio-loud and radio-quiet objects). We adopt the mean bolometric correction factor ($\text{BC}_V = 13.35$) at the V -band of radio-loud quasars drawn from Elvis et al. (1994) to calculate the bolometric luminosities for the objects in our sample. The V -band luminosities, for the objects in our sample, are computed from the luminosities of the g -band and r -band using the same method as Fukugita et al. (1996) and Véron-Cetty & Véron (2006). Figure 4 compares the integrated luminosities with the bolometric luminosities calculated from the V -band luminosities by multiplying them by the mean bolometric correction factor $\text{BC}_V = 13.35$. The figure clearly shows that the bolometric luminosities are still obviously smaller than the integrated luminosities. It indicates that the integrated luminosity can also not be estimated merely from the V -band luminosity by multiplying the mean bolometric correction factor $\text{BC}_V = 13.35$.

We notice that Elvis et al. (1994) have included only normal, nonblazar quasars. For the FSRQs, however, the orientation of jets is closer to the line of sight than that of normal quasars. Therefore, it is expectable that the contribution of the non-thermal emission from relativistic jets to all frequencies of FSRQs will be stronger than that of normal quasars.

Radio emission is usually used to represent jet emission. We estimate the radio luminosity at 5 GHz using the radio index between 1.4 GHz and 4.85 GHz. Then we perform the correlation between radio luminosities at 5 GHz and the departure between the integrated luminosities obtained by the integrated SED and the bolometric luminosities estimated by multiplying the continuum monochromatic luminosities at 5100 Å, 3000 Å and 1350 Å with the corresponding bolometric correction factors. The result is shown in Figure 5. We find that the departure strongly correlates with radio emission with a coefficient $r = 0.773$ at a significance level 10^{-9} for rejecting the null hypothesis of no correlation. This implies that the large value of the departure arises from the non-thermal emission of relativistic jets.

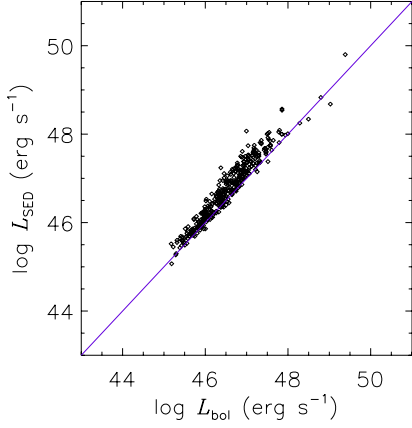


Fig. 4 L_{SED} versus L_{bol} values that are calculated by monochromatic luminosities at the V-band using a mean bolometric correction factor 13.35 of radio-loud quasars.

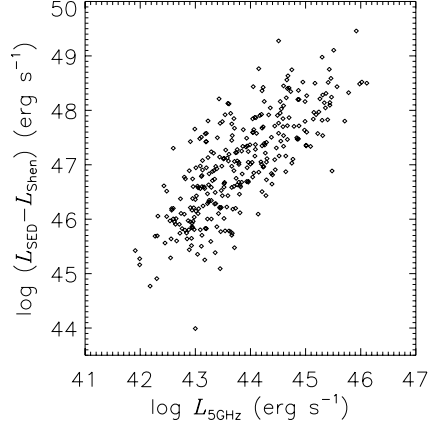


Fig. 5 Radio luminosities at 5GHz versus the departures between L_{SED} and L_{Shen} . The L_{Shen} are calculated by continuum monochromatic luminosities at 5100 Å, 3000 Å or 1350 Å, depending on redshift. The coefficient is 0.773 with a significance level of 10^{-9} for rejecting the null hypothesis of no correlation.

According to our analysis, we come to the conclusion that one cannot estimate the integrated luminosity by applying the bolometric correction factors of normal quasars to extremely radio-loud FSRQs. To estimate the integrated luminosity from the monochromatic luminosity, one might need an entirely new relation other than the conventional correction factors.

We investigate relations between the integrated luminosities and the monochromatic luminosities for FSRQs. The results are shown in Figure 6 and listed below.

The minimum χ^2 fitting for the integrated luminosities and monochromatic luminosities at radio 1.4 GHz gives

$$\log L_{\text{SED}} = (24.36 \pm 0.93) + (0.52 \pm 0.02) \log L_{1.4 \text{ GHz}}, \quad (2)$$

for 362 FSRQs with a coefficient $r = 0.791$ at a significance level 10^{-9} for rejecting the null hypothesis of no correlation. The minimum χ^2 fitting for the integrated luminosities and monochromatic luminosities at radio 4.85 GHz gives

$$\log L_{\text{SED}} = (17.97 \pm 1.07) + (0.65 \pm 0.02) \log L_{4.85 \text{ GHz}}, \quad (3)$$

for 362 FSRQs with a coefficient $r = 0.844$ at a significance level 10^{-9} for rejecting the null hypothesis of no correlation. The minimum χ^2 fitting for the integrated luminosities and monochromatic luminosities at the IR J band gives

$$\log L_{\text{SED}} = (-4.13 \pm 0.96) + (1.12 \pm 0.02) \log L_J, \quad (4)$$

for 286 FSRQs with a coefficient $r = 0.96$ at a significance level 10^{-9} for rejecting the null hypothesis of no correlation. The minimum χ^2 fitting for the integrated luminosities and monochromatic luminosities at the IR H band gives

$$\log L_{\text{SED}} = (-3.97 \pm 1.05) + (1.11 \pm 0.02) \log L_H, \quad (5)$$

for 239 FSRQs with a coefficient $r = 0.959$ at a significance level 10^{-9} for rejecting the null hypothesis of no correlation. The minimum χ^2 fitting for the integrated luminosities and monochromatic luminosities at the IR K band gives

$$\log L_{\text{SED}} = (-4.96 \pm 1.32) + (1.14 \pm 0.03) \log L_K, \quad (6)$$

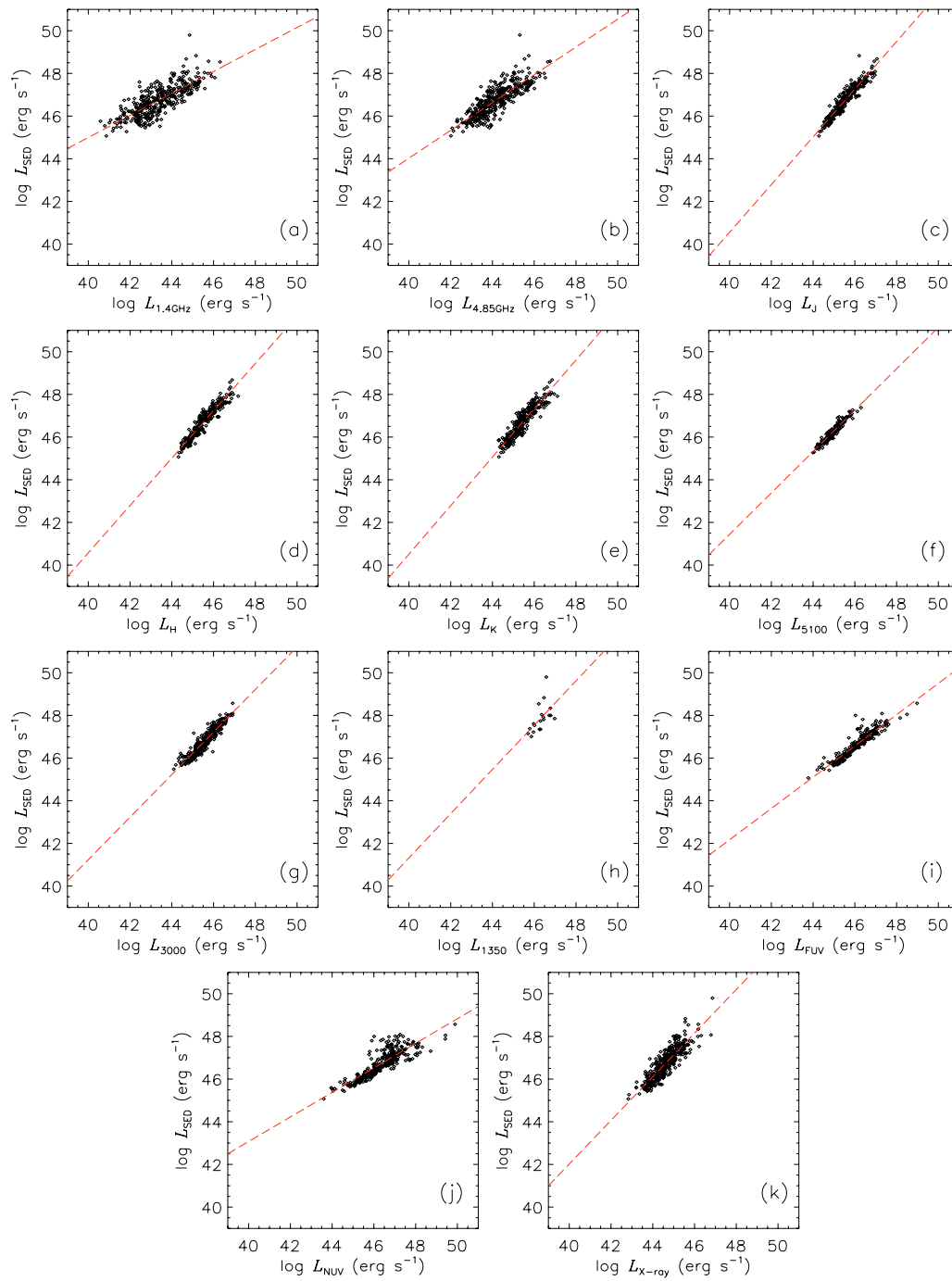


Fig. 6 L_{SED} versus monochromatic luminosities. The dashed lines are the minimum χ^2 fitting. (a) Radio luminosities at 1.4 GHz, (b) Radio luminosities at 4.85 GHz, (c) IR luminosities at J band, (d) IR luminosities at H band, (e) IR luminosities at K band, (f) Continuum monochromatic luminosities at 5100 Å, (g) Continuum monochromatic luminosities at 3000 Å, (h) Continuum monochromatic luminosities at 1350 Å, (i) UV luminosities at far-UV, (j) UV luminosities at near-UV, (k) X-ray luminosities at 2 keV.

for 260 FSRQs with a coefficient $r = 0.932$ at a significance level 10^{-9} for rejecting the null hypothesis of no correlation. The minimum χ^2 fitting for the integrated luminosities and monochromatic luminosities at 5100 \AA gives

$$\log L_{\text{SED}} = (2.64 \pm 1.16) + (0.97 \pm 0.03) \log L_{5100}, \quad (7)$$

for 132 FSRQs with a coefficient $r = 0.954$ at a significance level 10^{-9} for rejecting the null hypothesis of no correlation. The minimum χ^2 fitting for the integrated luminosities and monochromatic luminosities at 3000 \AA gives

$$\log L_{\text{SED}} = (1.36 \pm 1.03) + (1.00 \pm 0.02) \log L_{3000}, \quad (8)$$

for 286 FSRQs with a coefficient $r = 0.939$ at a significance level 10^{-9} for rejecting the null hypothesis of no correlation. The minimum χ^2 fitting for the integrated luminosities and monochromatic luminosities at 1350 \AA gives

$$\log L_{\text{SED}} = (-0.15 \pm 17.10) + (1.04 \pm 0.37) \log L_{1350}, \quad (9)$$

for 19 FSRQs with a coefficient $r = 0.716$ at a significance level 10^{-4} for rejecting the null hypothesis of no correlation. The minimum χ^2 fitting for the integrated luminosities and monochromatic luminosities at far-UV gives

$$\log L_{\text{SED}} = (12.85 \pm 0.86) + (0.73 \pm 0.02) \log L_{\text{FUV}}, \quad (10)$$

for 227 FSRQs with a coefficient $r = 0.945$ at a significance level 10^{-9} for rejecting the null hypothesis of no correlation. The minimum χ^2 fitting for the integrated luminosities and monochromatic luminosities at near-UV gives

$$\log L_{\text{SED}} = (20.05 \pm 0.96) + (0.58 \pm 0.02) \log L_{\text{NUV}}, \quad (11)$$

for 295 FSRQs with a coefficient $r = 0.864$ at a significance level 10^{-9} for rejecting the null hypothesis of no correlation. The minimum χ^2 fitting for the integrated luminosities and monochromatic luminosities at X-ray 2 keV gives

$$\log L_{\text{SED}} = (1.14 \pm 1.34) + (1.02 \pm 0.03) \log L_{\text{X-ray}}, \quad (12)$$

for 362 FSRQs with a coefficient $r = 0.886$ at a significance level 10^{-9} for rejecting the null hypothesis of no correlation.

We call Equations (2)–(12) empirical relations that can estimate integrated luminosities of FSRQs from different monochromatic luminosities. We believe that using Equations (2)–(12) to estimate integrated luminosities of FSRQs from monochromatic luminosities should be more reliable than merely multiplying the latter by the bolometric correction factors drawn from normal, nonblazar quasars, which is what has been done previously.

It should be pointed out that from our empirical relations, one can estimate the integrated luminosity from the corresponding monochromatic luminosity. This does not suggest that the integrated luminosity obtained can represent the bolometric luminosity of FSRQs since the integrated luminosity must be influenced by the beaming effect. It is desired that when more data are available, the role of the beaming effect of FSRQs in this aspect can be plainly revealed and the intrinsic physical properties of the relation can be well understood.

Acknowledgements This work was supported by the National Natural Science Foundation of China (Grant No. 10847003).

References

- Anderson, S. F., et al. 2007, *AJ*, 133, 313
- Budavári, T., et al. 2009, *ApJ*, 694, 1281
- Chen, Z., Gu, M., & Cao, X. 2009, *MNRAS*, 397, 1713
- Edelson, R. A., & Malkan, M. A. 1986, *ApJ*, 308, 59
- Elvis, M., et al. 1994, *ApJS*, 95, 1
- Fukugita, M., Ichikawa, T., Gunn, J. E., Doi, M., Shimasaku, K., & Schneider, D. P. 1996, *AJ*, 111, 1748
- Gregory, P. C., Scott, W. K., Douglas, K., & Condon, J. J. 1996, *ApJS*, 103, 427
- Kaspi, S., Smith, P. S., Netzer, H., Maoz, D., Jannuzi, B. T., & Giveon, U. 2000, *ApJ*, 533, 631
- Kimball, A. E., & Ivezić, Ž. 2008, *AJ*, 136, 684
- Kim, M., Ho, L. C., Peng, C. Y., Barth, A. J., Im, M., Martini, P., & Nelson, C. H. 2008, *ApJ*, 687, 767
- Kollmeier, J. A., et al. 2006, *ApJ*, 648, 128
- Lu, Y., Wang, T.-G., Dong, X.-B., & Zhou, H.-Y. 2010, *MNRAS*, 404, 1761
- Maiolino, R., Salvati, M., Marconi, A., Antonucci, R. R. J. 2001, *A&A*, 375, 25
- Martin, D. C., et al. 2005, *ApJ*, 619, L1
- Mas-Hesse, J. M., Rodriguez-Pascual, P. M., Sanz Fernandez de Cordoba, L., Mirabel, I. F., Wamsteker, W., Makino, F., & Otani, C. 1995, *A&A*, 298, 22
- McLure, R. J., & Dunlop, J. S. 2004, *MNRAS*, 352, 1390
- Miller, L., Peacock, J. A., & Mead, A. R. G. 1990, *MNRAS*, 244, 207
- Netzer, H. 2003, *ApJ*, 583, L5
- Netzer, H. 1990, *Active Galactic Nuclei*, ed. R. D. Blandford, H. Netzer, & L. Woltjer (Berlin: Springer), 57
- Peterson, B. M. 1997, *An introduction to active galactic nuclei*, Publisher: Cambridge, New York Cambridge University Press, 1997 Physical description xvi, 238 p. ISBN 0521473489,
- Peterson, B. M., et al. 2004, *ApJ*, 613, 682
- Richards, G. T., et al. 2006, *ApJS*, 166, 470
- Sambruna, R. M., Maraschi, L., & Urry, C. M. 1996, *ApJ*, 463, 444
- Sanders, D. B., Phinney, E. S., Neugebauer, G., Soifer, B. T., & Matthews, K. 1989, *ApJ*, 347, 29
- Schlegel, D. J., Finkbeiner, D. P., & Davis, M. 1998, *ApJ*, 500, 525
- Schmitt, H. R., Kinney, A. L., Calzetti, D., & Storchi Bergmann, T. 1997, *AJ*, 114, 592
- Schneider, D. P., et al. 2007, *AJ*, 134, 102
- Schneider, D. P., et al. 2010, *AJ*, 139, 2360
- Shen, Y., Greene, J. E., Strauss, M. A., Richards, G. T., & Schneider, D. P. 2008, *ApJ*, 680, 169
- Skrutskie, M. F., et al. 2006, *AJ*, 131, 1163
- Spergel, D. N., et al. 2007, *ApJS*, 170, 377
- Stark, A. A., Gammie, C. F., Wilson, R. W., Bally, J., Linke, R. A., Heiles, C., & Hurwitz, M. 1992, *ApJS*, 79, 77
- Sun, W.-H., & Malkan, M. A. 1989, *ApJ*, 346, 68
- Urry, C. M., & Padovani, P. 1995, *PASP*, 107, 803
- Véron-Cetty, M.-P., & Véron, P. 2006, *A&A*, 455, 773
- Ward, M., Elvis, M., Fabbiano, G., Carleton, N. P., Willner, S. P., & Lawrence, A. 1987, *ApJ*, 315, 74
- Warner, C., Hamann, F., & Dietrich, M. 2004, *ApJ*, 608, 136
- White, R. L., Becker, R. H., Helfand, D. J., & Gregg, M. D. 1997, *ApJ*, 475, 479
- Woo, J.-H., & Urry, C. M. 2002, *ApJ*, 579, 530
- Woo, J.-H., Treu, T., Malkan, M. A., & Blandford, R. D. 2006, *ApJ*, 645, 900
- Wu, Q. 2009, *MNRAS*, 398, 1905
- Wu, X.-B., Wang, R., Kong, M. Z., Liu, F. K., & Han, J. L. 2004, *A&A*, 424, 793
- Wu, X.-B., & Liu, F. K. 2004, *ApJ*, 614, 91